

Available online at [www.sciencedirect.com](http://www.sciencedirect.com)**SciVerse ScienceDirect**

Procedia Engineering 42 (2012) 1189 – 1201

**Procedia  
Engineering**[www.elsevier.com/locate/procedia](http://www.elsevier.com/locate/procedia)

20<sup>th</sup> International Congress of Chemical and Process Engineering CHISA 2012  
25 – 29 August 2012, Prague, Czech Republic

## Model-based investigation of a pellet string reactor

A. Müller, J. Petschick, R. Lange a\*

*Institute of Process Engineering and Environmental Technology, Chair of Chemical Reaction Engineering and Process Plant,  
Technische Universität Dresden, 01062 Dresden, DE*

---

### Abstract

By means of numerical modeling, the behavior of chemical reactors for multiphase reactions can be predicted and the experimental effort can be reduced to a minimum. A Pellet String Reactor for a heterogeneously catalyzed reaction has been investigated based on a model built with the CFD software COMSOL Multiphysics® 4.2a [1]. Pressure drop and residence time distribution studies were performed to evaluate the reactor design regarding its hydrodynamic characteristics. The influence of the fluid velocity is discussed as well as the model dimension. For an estimation of the hydrodynamic characteristics a 2D model was regarded as sufficient.

© 2012 Published by Elsevier Ltd. Selection under responsibility of the Congress Scientific Committee (Petr Kluson) Open access under [CC BY-NC-ND license](https://creativecommons.org/licenses/by-nc-nd/4.0/).

*Keywords:* CFD model; hydrodynamics; multi-phase reaction; pellet string reactor; fixed bed

---

### 1. Introduction

Heterogeneous catalysis plays an important role in the production of fine chemicals and intermediates. Therefore a constant effort to optimize the use of the catalysts in order to decrease the process costs is present. Furthermore the current trend is from batch to continuous production processes, which are often more effective and deliver a constantly high product quality. Typically fixed bed reactors are employed, operated with catalyst pellets in the size of 2 – 6 mm. Their design and operation is very complex, especially when gas and liquid are present as fluids. For performance evaluation and screening of optimal process conditions in gas-liquid-solid reactions, a single pellet string reactor can be a suitable tool.

---

\* Corresponding author. Tel.: +49-351-463-35181; fax: +49-351-463-37757.

*E-mail address:* [ruediger.lange@tu-dresden.de](mailto:ruediger.lange@tu-dresden.de).

## Nomenclature

$Bo$	Bodenstein number [-]
$c$	concentration [ $mol/m^3$ ]
$d$	particle diameter [ $m$ ]
$D$	channel diameter [ $m$ ]
$D_L$	diffusion coefficient of the fluid [ $m^2/s$ ]
$D_{ax}$	axial dispersion coefficient [ $m^2/s$ ]
$f_{bed}$	bed friction factor [-]
$g$	gravitational acceleration [ $m/s^2$ ]
$K_{1,2}$	constants for friction factor [-]
$L$	bed length [ $m$ ]
$p$	pressure [ $Pa$ ]
$\Delta p$	pressure drop [ $Pa$ ]
$r$	reaction rate [ $mol/(m^3 \cdot s)$ ]
$Re_{bed}$	bed Reynolds number [-]
$t$	time [ $s$ ]
$T$	temperature [ $K$ ]
$u_0$	superficial velocity [ $m/s$ ]
$\vec{u}$	velocity vector [ $m/s$ ]
$z$	axial distance from reactor inlet [ $m$ ]

### Greek letters

$\varepsilon_{bed}$	bed porosity [-]
$\eta$	viscosity [ $Pa \cdot s$ ]
$\rho$	density [ $kg/m^3$ ]
$\sigma$	surface tension [ $N/m$ ]
$\tau$	mean residence time [ $s$ ]
$\nu$	stoichiometric coefficient [-]

### Acronyms

AMS	alpha-methylstyrene
CFD	computational fluid dynamics
FEM	finite element method
RTD	residence time distribution

### 1.1. Pellet string reactor concept

The investigation of optimal reaction conditions for gas-liquid-solid-reactions plays an important role regarding an economical and ecological process design. These parameters are preferably identified during lab-scale experiments to save time and resources. On the other hand these conditions have to be measured with great care and in a suitable reactor setup that allows an easy scale-up, because of the large impact in the later process. Such a setup ideally allows a direct control of the flow conditions at the catalyst particle and ensures constant conditions for all particles. The catalyst packing needs to be reproducible and any changes regarding the catalyst structure should be instantaneously detectable. Furthermore easy control of the thermal state is necessary, e.g. to maintain isothermal conditions. Many of these features are combined in the pellet string reactor concept. This concept comprises a tube reactor, filled with catalyst particles which are only slightly smaller than the tube diameter. The dimension is most often between 2

and 10 mm in diameter and up to several meters in length. The tube can be in vertical, horizontal or spiral arrangement with either a round or a square cross-section.

As the wall surface to volume ratio is much higher than in traditional fixed beds, heat management is improved and a more isothermal operation can be expected. Due to the almost linear arrangement, the particles are in close contact with the gas and liquid phase. A formation of flow channels and wall effects, as occurring in larger fixed beds, can be eliminated. Therefore the chemical reaction conditions are expected to be equal for each particle. Nonetheless, hydrodynamic conditions should be investigated, for example by CFD modeling and visual studies in transparent channels, to discover all important effects.

The concept of the pellet string reactor has been well-known for a long time and has been employed for measuring mass transfer coefficients and kinetics, mostly in gas-phase reactions [2-8]. Works on gas-liquid-solid applications are rarer. A pellet string of large particles (8.2 mm) was employed by Satterfield [9] to investigate mass transfer limitations for the hydrogenation of alpha-methylstyrene to cumene. More recent publications on catalyst screening in a pellet string reactor were published by Papayannakos et al. [10-12] and Hipolito et al. [13-14], who also presented detailed hydrodynamic specifications.

### *1.2. Study objectives*

The CFD studies serve to identify the hydrodynamic characteristics of a pellet string reactor. Hydrodynamics include all effects related to fluid flow through the fixed bed reactor. They are of particular importance for gas-liquid-solid reaction due to the significant impact on mass and heat transfer. Main factors influencing the state of flow are the fluid properties (e.g. density, viscosity, surface tension), the fluid velocity (gas and/or liquid), the liquid hold-up and the reactor geometry (e.g. reactor diameter, particle diameter, diameter ratio). Two very common parameters describing fluid dynamics are the pressure drop and the residence time distribution (RTD). The former is a major design parameter for process plants as it determines a significant part of the energy balance and therefore the operating efficiency. The latter gives information about the plug flow behavior and the presence of dead zones, which can be problematic in terms of conversion and selectivity [15]. In this paper, the influence of fluid velocity and reactor geometry will be discussed for a defined fluid system, based on a 2D approximation of the reactor for single-phase flow. A first approach to the comparison with a 3D model will also be given. In addition the details of setting up the CFD model are presented. The overall aim is the implementation of a hydrodynamic reactor model serving as a base for further extension with reaction kinetics for a full reactor model and as a comparison to experimental data.

### *1.3. Fluid system*

Studies were performed with a single-phase liquid. A model system of alpha-methylstyrene (AMS) and cumene, both aromatic hydrocarbons, was implemented. It is assumed that cumene has the same properties as AMS as presented in Table 1. For residence time studies a tracer substance is used, i.e. an increased concentration of AMS. As AMS has very similar properties to cumene but can be detected in the mixture by a different refractive index this method is also suitable for experimental validations later on. Furthermore the hydrogenation of AMS to cumene over a palladium catalyst can be modeled in subsequent investigations by adding dissolved hydrogen to the liquid.

Table 1. Material properties of the fluid [16]

Material	$T [K]$	$p [Pa]$	$\rho [kg/m^3]$	$\eta [Pa\cdot s]$	$\sigma [N/m]$	$D_L [m^2/s]$
AMS / cumene	298	$10\cdot 10^5$	899.4	$0.85\cdot 10^{-3}$	$28.0\cdot 10^{-3}$	$9.8\cdot 10^{-9}$

## 2. CFD model

CFD has proven to be a powerful tool to model the flow behavior and performance of chemical reactors. In order to study the hydrodynamic characteristics of a pellet string reactor the commercial CFD software COMSOL Multiphysics<sup>®</sup> 4.2a was employed. The program presents a platform to solve the differential equations of the Navier-Stokes equations in combination with component material balances by means of the finite element method (FEM).

### 2.1. Model setup

A pellet string reactor geometry was investigated in the CFD model. A round channel with a diameter of 4 mm was filled with spheres with a mean diameter of 3.33 mm, representing catalyst particles. In addition a similar geometry was built for a 2.4 mm channel with 2 mm spheres. Drawings of the geometry are depicted in Fig. 1. The bed porosity  $\varepsilon_{bed}$  was estimated based on geometrical considerations according to the correlation of Dixon [17]. For the investigations a 2D model and a 3D model were built. Although a 2D model does not represent the 3D structure completely, it can still give a first idea about the effects inside the channel. However, the 2D geometry was adjusted by an increased distance between the spheres to allow fluid flow. To keep the computational effort reasonable, the bed length was set to 0.1 m for the 2D model and to 0.02 m for the 3D model. Due to the irregular structure of the bed the use of symmetry axes to simplify the model was not applicable.

Based on the CFD model, the effect of geometry and fluid velocity on residence time distribution and pressure drop will be discussed (Table 2).

Table 2. Parameter ranges for simulation studies.

$T [K]$	$p [Pa]$	$d [m]$	$D [m]$	$D/d [-]$	$L [m]$	$\varepsilon_{bed} [-]$	$u_0 [m/s]$	$Re_{bed} [-]$
298.0	$10\cdot 10^5$	$2.0\cdot 10^{-3}$ , $3.33\cdot 10^{-3}$	$2.4\cdot 10^{-3}$ , $4.0\cdot 10^{-3}$	1.2	0.1	0.53	0.001...0.25	4.5...1870

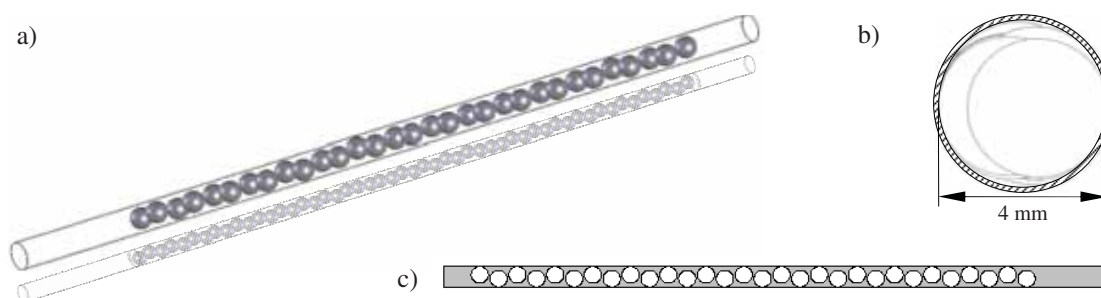


Fig. 1. Geometry of the reactor model a) 3D model for  $D = 4$  mm and  $D = 2.4$  mm, b) 2D cross-sectional view, c) 2D model for  $D = 4$  mm channel

## 2.2. Model equations

Numerical simulation of fluid flow is based on the laws of conservation for mass, momentum and energy. In the simulation single-phase liquid flow was investigated. The CFD model for hydrodynamic studies is based on a  $k$ - $\varepsilon$ -model for stationary turbulent flow in combination with a time-dependent mass transport model. For the lowest velocity  $u_0 = 0.001$  m/s a laminar flow model was applied. Mass transport is described through convection and diffusion, where the viscosity from the  $k$ - $\varepsilon$ -model describes the species diffusion in the mass transport. To simplify the corresponding system of differential equations, the following assumptions were made:

- isothermal system
- incompressible fluid
- Newtonian fluid
- similar material properties of AMS and cumene.

### 2.2.1. Momentum balance

Based on the assumptions, the system of equations is reduced to the continuity equation for the overall mass balance (1) and the Navier-Stokes equation for the momentum balance (2) [18]. The energy balance can be neglected for isothermal conditions prevail.

$$\rho \cdot \nabla \bar{u} = 0 \quad (1)$$

$$\rho \frac{\partial \bar{u}}{\partial t} + \rho \cdot (\bar{u} \cdot \nabla) \bar{u} = -\nabla p + \eta \cdot \nabla^2 \bar{u} + \rho \cdot g \quad (2)$$

Due to the spheres inside the channel, the flow inside the reactor can be considered as turbulent for a fluid velocity exceeding  $u_0 = 0.0015$  m/s. This is indicated by the Reynolds number for packed beds  $Re_{bed}$  (3). The critical Reynolds number for the transition from laminar to turbulent is approximately 10 [19]. In the considered velocity range, the bed Reynolds number ranges from approximately 4.5 up to 1870, thus indicating laminar flow for the lowest velocity and the turbulent regime for the remaining.

$$Re_{bed} = \frac{\rho \cdot u_0 \cdot d}{\eta \cdot (1 - \varepsilon_{bed})} \quad (3)$$

Describing turbulent flow with the Navier-Stokes equations is quite difficult, as a turbulent system covers a wide range of scales in the flow. To solve the equation system for all scales (Direct Numeric Simulation, DNS) would cause an immense amount of data and is in most cases not reasonable. It is more practicable to simplify the calculations by modeling only average values without the resolution of turbulences [18]. In this case the Reynolds averaged Navier-Stokes (RANS) equations are used to solve for the pressure and the mean velocity profile, which implies time averaging of the velocity fluctuations in turbulent flow. In addition a turbulence model, the  $k$ - $\varepsilon$ -model, is employed to describe the Reynolds stresses of the RANS approach. This model introduces two additional transport equations and two dependent variables: the turbulent kinetic energy,  $k$ , and the dissipation rate of turbulence energy,  $\varepsilon$ . The second variable can be thought of as the variable that determines the length-scale of the turbulence, whereas the first variable,  $k$ , determines the energy in the turbulence. More details on the turbulence model can be found in the literature [18].

### 2.2.2. Component Material Balances

In addition to the overall mass balance for the system (continuity equation), material balances for each

component are required to describe the local concentration profiles for the RTD. As the tracer is present in diluted form, the COMSOL method “Transport of diluted species” (Chemical Reaction Engineering Module) can be applied, which includes diffusion and convection to model the component concentrations in the fluid and considers fluid properties as constant. The material balance based on the amount of substance is generally expressed by equation (4) [18].

$$\frac{\partial c_i}{\partial t} = \nabla(D_{L,i} \nabla c_i) - \bar{u} \nabla c_i + \sum_{i,j} v_i r_{i,j} \tag{4}$$

For studying the RTD it is assumed that no reaction takes place, therefore the term describing the change in concentration due to chemical reaction disappears (5).

$$\frac{\partial c_i}{\partial t} + \nabla \cdot (-D_{L,i} \nabla c_i + c_i \cdot \bar{u}) = 0 \tag{5}$$

To solve the overall space-dependent model, the equations of motion and the material balance equations are coupled and solved for velocity, concentration and pressure.

### 2.3. Boundary conditions

In order to solve a system of differential equations, initial and boundary conditions have to be given. In the model different boundaries are present and each boundary should be specified by one boundary condition for the mass and the momentum balance [18].

At the inlet usually Dirichlet boundary conditions are specified, as the system parameters are known or can be estimated easily. Here the inlet velocity  $u_0$  and concentration  $c_0$  were defined. A time dependent concentration function was implemented to model the tracer pulse (6) for the residence time studies.

$$c(t) = c_0 \exp^{-(t-3)^2} \tag{6}$$

The outlet boundary conditions are evidently harder to estimate. The velocity can be defined by an outlet pressure, due to the connection of velocity and pressure in the continuity and Navier-Stokes equation [18]. For the concentration it is assumed that mass transfer is only caused by convection in the free flowing fluid.

Regarding hydrodynamics the walls of the channel and the surface of the spheres are impermeable walls and are modeled using a wall function. This is necessary to describe the “no-slip” condition at the wall for turbulent flow modeled with the  $k-\epsilon$ -model. A wall function is employed to model the thin region near the wall with high gradients in the flow variables based on a logarithmic approach. More details on the wall function are presented in [20]. When it comes to the material balances of the convection and diffusion model the channel walls and the spheres present boundaries with an insulating condition. A summary of the boundary conditions is presented in Table 3.

Table 3. Boundary and subdomain conditions for the CFD model

	<i>inlet</i>	<i>outlet</i>	<i>channel wall</i>	<i>catalyst pellet wall</i>	<i>free fluid</i>
momentum balance	$u_0$	$p_0$	wall function	wall function	Navier-Stokes
component mass balance	$c_0$	convective flux	no flux	no flux	convection and diffusion

## 2.4. Mesh generation

The partial differential equations that govern fluid flow and heat transfer can usually not be solved analytically. Therefore the flow domains are split into smaller cells for which the governing equations are discretized and solved numerically. In this work a mesh structure based on triangles (2D) and tetrahedra (3D) was used, which is also one of the most common mesh forms for complex geometries [20].

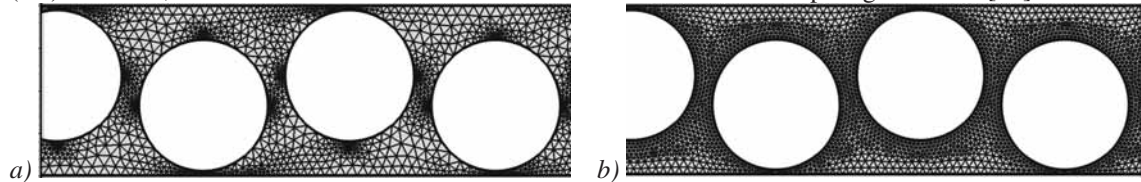


Fig. 2. Mesh geometry for the simulation of a) the turbulent flow (stationary) and b) the mass transport through convection and diffusion (time-dependent)

COMSOL provides a mesh generation tool that automatically refines the mesh in domains with higher calculation accuracy requirements, like areas of increased turbulence and chemical reaction. In addition the mesh dimensions were specified separately for stationary turbulent flow and time-dependent tracer simulation. As the numerical solution is only obtained at the mesh points, the simulation result becomes more accurate with increasing fineness of the mesh (i.e. increasing cell number). Especially transient mass transfer processes require a very fine mesh in order to obtain a reasonable solution. On the other hand the computational time increases strongly with a finer mesh. Therefore it is applicable to use different mesh geometries for the simulation. A rather coarse mesh is used for a stationary solution of the turbulent flow based on the  $k-\varepsilon$  model (Fig. 2a)). In addition a finer mesh is generated for the calculation of the time-dependent mass transfer (Fig. 2b)). Both calculation steps are coupled by the turbulent viscosity from the  $k-\varepsilon$  model that describes the diffusion process. This approach reduces computational time while still providing an accurate solution.

A mesh size variation was performed in order to determine the necessary degree of fineness. The mesh was refined or enlarged until the calculation results remained constant. Furthermore the quality of the mesh was checked. The final mesh parameters of the 2D model are summarized in Table 4.

Table 4. Parameters for the stationary and the time dependent mesh of the 2D model

Mesh		1 (stationary)	2 (time-dependent)
Channel	max. cell size [mm]	2.0	0.2
	min. cell size [mm]	0.01	$6.0 \cdot 10^{-4}$
wall region	max. cell size [mm]	0.04	0.1
	min. cell size [mm]	0.01	$6.0 \cdot 10^{-4}$
number of elements		20042	38386

Special attention was paid to the mesh structure close to the walls to model the laminar sublayer developing in the region of turbulent flow near a no-slip boundary. Because of the decrease in flow velocity towards the no-slip boundary, the Reynolds number decreases until at some point the flow crosses the threshold from turbulent to laminar. Thus the region near the walls needs to have a fine mesh resolution and a dedicated wall model is used by COMSOL. The thickness of the sublayer,  $\delta_w$  (also called wall lift-off), is estimated by COMSOL so that the viscous wall lift-off  $\delta_w^+$  becomes 11.06. A higher value indicates that the mesh is too coarse. In the presented model a value of 11.06 was reached and  $\delta_w$  is also small compared to the geometry of the reactor.



### 3. Results and Discussion

The presented CFD model was employed to perform simulation studies for the pressure drop and the residence time distribution. The velocity profiles already show some stagnant zones between the particles

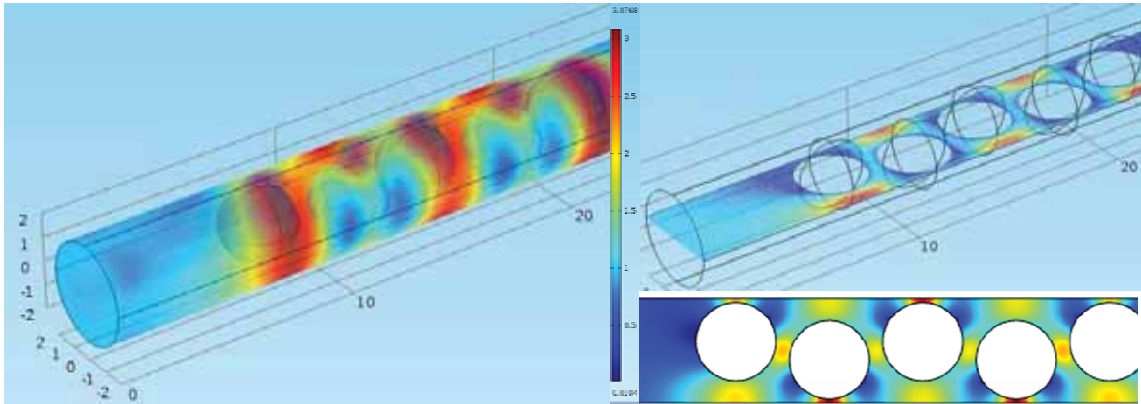


Fig. 3. Velocity field [ $10^{-3}$  m/s] inside the reactor ( $D = 4$  mm, liquid: water) in the 3D and 2D model, stagnant zones around the spheres appear in dark blue

and the wall and areas of increase fluid velocity in the main passage stream for the 2D as well as for the 3D model (Fig. 3).

#### 3.1. Pressure drop

The pressure drop presents a measure for the flow resistance inside a channel and is a major design parameter for processes. As shown in Fig. 4a), the pressure drop increases with increasing fluid velocity due to the higher friction forces between the fluid and the particles.

The pressure drop in a packed reactor can be described with the well-known Ergun equation. This model describes the frictional pressure drop as a contribution of laminar and turbulent effects [21]. When the diameter ratio  $N=D/d$  falls below  $N=10$ , the effect of the confining wall increases and therefore the correlation becomes less accurate. Several authors have investigated this problem for single-phase flow and developed modified equations to predict the pressure drop in packed tubes with low tube-to-particle-diameter ratios [22-27]. The simulation results were compared to two pressure drop correlations. Both of them present modifications of the Ergun equation for the pressure drop  $\Delta p$  over a certain bed length  $L$  with the friction factor  $f_{bed}$  (7).

$$\frac{\Delta p}{L} = f_{bed} \cdot \left( \frac{1 - \varepsilon_{bed}}{\varepsilon_{bed}^3} \right) \cdot \frac{\rho \cdot u_0^2}{d} \cdot \left( 1 + \frac{2}{3 \cdot (1 - \varepsilon_{bed})} \frac{d}{D} \right) \quad (7)$$

$$f_{bed} = \frac{K_1}{\text{Re}_{bed}} + K_2 \quad (8)$$

One correlation was developed by Reichelt [22], whereas the other one is a more recent modification of Cheng [27]. Cheng developed a more detailed estimation for  $K_1$  based on the bed geometry and also improved the estimation of  $K_2$ . More details are presented in Appendix A.



The results for the pressure drop generated with the 2D model in COMSOL fit well with the two correlations, as shown in Fig. 4a). This applies for the velocity dependence as well as for the diameter variation. The model accounts for the increase in pressure drop caused by a higher fluid velocity and a decreased particle size. However, the pressure drop of the 2D model depends strongly on the chosen geometry regarding the arrangement of the bed and the distance between spheres and the wall. Investigations on a representative 2D geometry are still ongoing and only a first estimation was used.

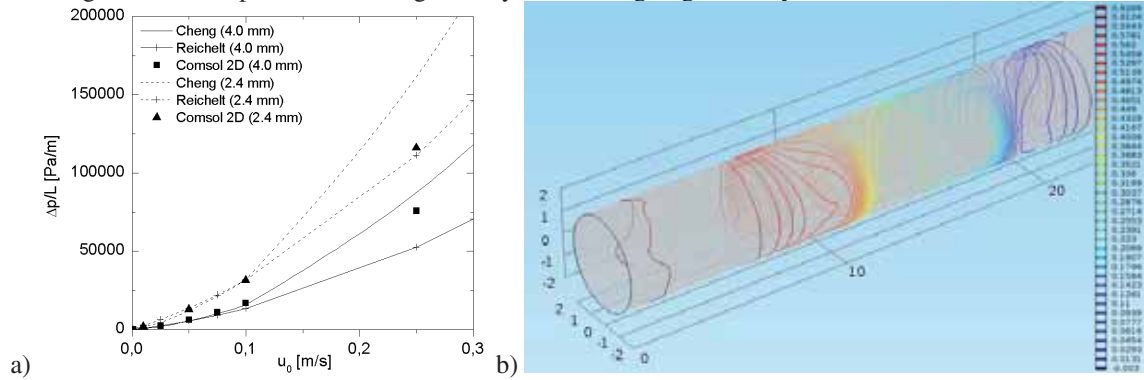


Fig. 4. a) Pressure drop vs. fluid velocity for both bed geometries, b) 3D model with isobars indicating the pressure drop ( $\Delta p$  [Pa])

First results from the 3D model showed similar results (Fig. 4b)). Nevertheless these results need to be verified for different velocities with an extended model.

### 3.2. Residence time distribution

The performance of a chemical reactor is strongly influenced by the residence time of the molecules. Having a large residence time variation, conversion is affected by backmixing and cannot be predicted very well. In this work, a tracer pulse of AMS is injected at the inlet of the reactor and the concentration is monitored at the outlet and also along the bed. The curves in Fig. 5 represent the concentration over time at the inlet and outlet, as well as at two points in the bed. For both velocities a well developed plug flow behavior is noticeable. This is indicated by a symmetric and relatively narrow concentration profile. A slight tailing of the concentration can be explained by stagnant zones between the particles which retain the tracer longer. The fluid velocity does not seem to have a significant influence, although an increased velocity somewhat yields improved plug flow. Further studies at higher velocity are currently being prepared to confirm this effect. This also corresponds to results published by Kallinikos et al. [10].

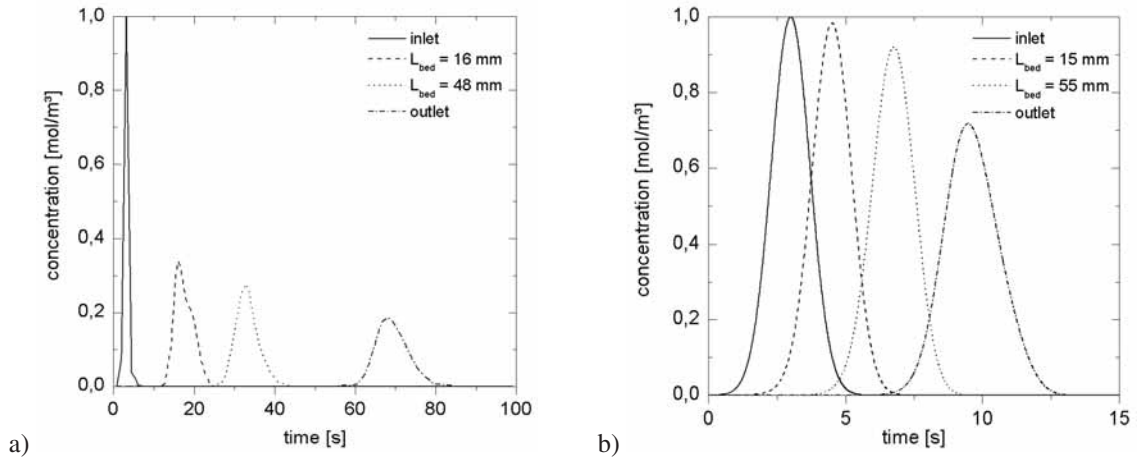


Fig. 5. Tracer concentration curves over reactor length at a)  $u_0 = 0.001$  m/s and b)  $u_0 = 0.01$  m/s

A conventional axial dispersion model was applied to the concentration profiles to estimate the Bodenstein number ( $Bo$ ) (eq. (9)). Two points in the bed were taken as references and a model with open boundaries regarding dispersion was assumed. The Bodenstein number describes the ratio of convective to diffusive processes and presents a good measure to evaluate plug flow behavior [15]. The obtained results deliver values of about 220 to 290 (Table 5), thus indicating well-developed plug flow ( $Bo > 100$ ).

$$\frac{\partial c}{\partial t} = D_{ax} \frac{\partial^2 c}{\partial z^2} - u_0 \frac{\partial c}{\partial z} \quad (9)$$

$$Bo = \frac{u_0 \cdot L}{D_{ax}} \quad (10)$$

Table 5. Mean residence time and Bodenstein number estimated with the 2D model for two different fluid velocities ( $D = 4.0$  mm)

$u_0$ [m/s]	0.001	0.01
$\tau$ [s]	69.2	6.8
$Bo$ [-]	220.7	290.7

First RTD studies were also performed in a 3D model for a short bed. Fig. 6 depicts how the tracer concentration pulse moves through the packed channel and gets dispersed. Simulations for the velocity variation with a longer bed are in preparation. Extending the length of the bed will improve the comparability to results from literature and experimental data.

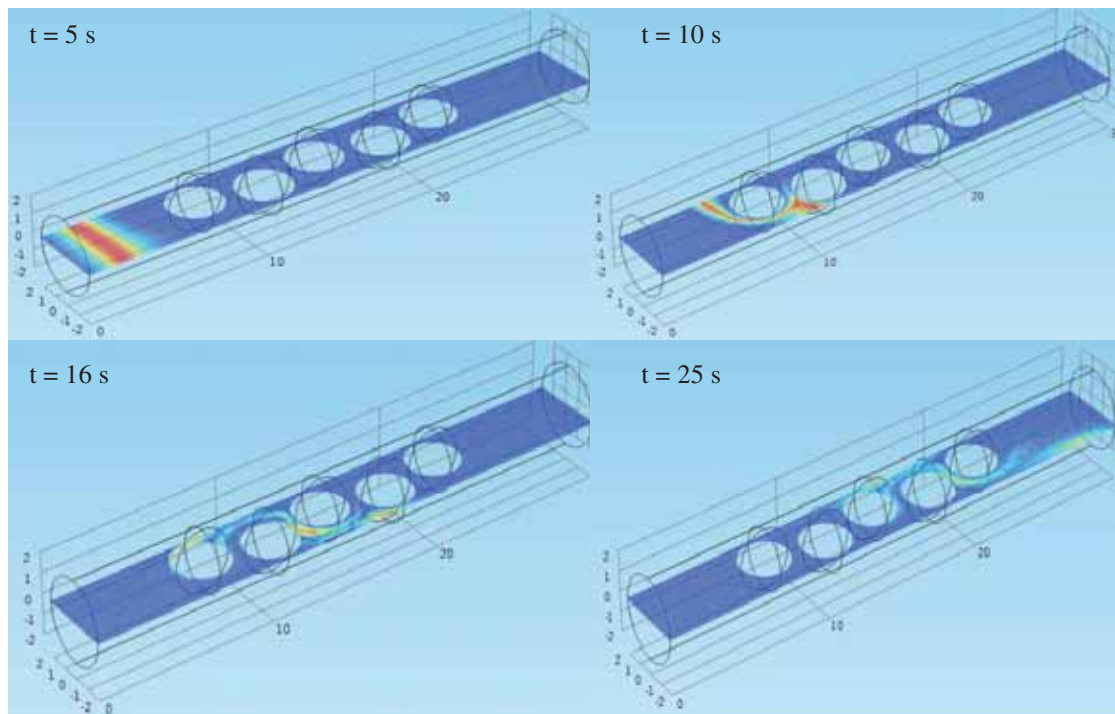


Fig. 6. Time-dependent tracer concentration distribution ( $D = 4.0$  mm,  $u_0 = 0.001$  m/s, 3D model)

#### 4. Conclusions

A numerical model was developed for the hydrodynamic investigation of a pellet string reactor with single-phase flow in COMSOL Multiphysics® 4.2a. Pressure drop and RTD studies were performed. Simulations were mainly carried out in a 2D model with a few orienteering simulations in a 3D model. The simplifications of the 2D model were considered acceptable for estimation of the hydrodynamic behavior as the model reflects the characteristics sufficiently. The pressure drop depends on fluid velocity and reactor geometry and corresponds well to established pressure drop models. The RTD studies have shown that a well-developed plug flow is obtained almost independently of the fluid velocity. For further comparison more parameter variations and an extended 3D model, covering a broader reactor length, will be applied in the near future.

The model serves as a basis for further investigations on the hydrodynamics in the pellet string reactor. In addition experimental studies will be performed to validate the numerical simulations. Moreover the reactor model will be expanded by combining hydrodynamics and reaction kinetics for the hydrogenation of AMS. Further improvements of the model could include a heat balance and the implementation of more complex kinetics. A long term objective would be the implementation of a second fluid phase to model a gas-liquid flow through the bed. Finally the reactor model could be employed as a versatile tool to determine the optimal reactor design and process parameters for selected hydrogenation reactions.

#### Acknowledgements

The authors thank the Bundesministerium für Bildung und Forschung (BMBF) for financial support

within the project “ $\mu$ RT.lab – Mikroreaktionstechnik für die chemische Industrie” (03FO3192).

## References

- [1] Licence number 1035438. Technische Universität Dresden, ZIH. 2012.
- [2] Scott DS, Lee W, Papa J. Measurement of transport-coefficients in gas-solid heterogeneous reactions. *Chem Eng Sci* 1974;**29**:2155-67.
- [3] Lee MD, Shen SH, Chung TK, Kuei CK. Flow and Dispersive Behaviors of Cylindrical Pellet String Reactor. *Aiche J* 1984;**30**:639-41.
- [4] Sharma RK, Cresswell DL, Newson EJ. Effective diffusion-coefficients and tortuosity factors for commercial catalysts. *Ind Eng Chem Res* 1991;**30**:1428-33.
- [5] Solcova O, Schneider P. Axial-dispersion in single-pellet-string columns packed with cylindrical particles. *Chem Eng Sci* 1994;**49**:401-8.
- [6] Takacs K, Calis HP, Gerritsen AW, VanDenBleek CM. The selective catalytic reduction of nitric oxide in the bead string reactor. *Chem Eng Sci* 1996;**51**:1789-98.
- [7] Tottrup PB. Evaluation of intrinsic steam reforming kinetic-parameters from rate measurements on full particle-size. *Appl Catal* 1982;**4**:377-89.
- [8] Solcova O, Soukup K, Schneider P. Diffusion coefficients and other transport characteristics of peculiarly shaped porous materials in the single pellet-string column. *Micropor Mesopor Mat* 2006;**91**:100-6.
- [9] Satterfield CN, Pelossof AA, Sherwood TK. Mass transfer limitations in a trickle-bed reactor. *Aiche J* 1969;**15**:226-34.
- [10] Kallinikos LE, Papayannakos NG. Fluid dynamic characteristics of a structured bed spiral mini-reactor. *Chem Eng Sci* 2007;**62**:5979-88.
- [11] Kallinikos LE, Papayannakos NG. Operation of a miniscale string bed reactor in spiral form at hydrotreatment conditions. *Ind Eng Chem Res* 2007;**46**:5531-5.
- [12] Patent: Bellos G, Galtier P, Papayannakos N, inventors; assignee. *Laboratory reactor for studying gaseous and liquid phase reactions*. US20070071664A1. 2007.
- [13] Hipolito AI, Rolland M, Boyer C, de Bellefon C. Single Pellet String Reactor for Intensification of Catalyst Testing in Gas/Liquid/Solid Configuration. *Oil Gas Sci Technol* 2010;**65**:689-701.
- [14] Vonortas A, Hipolito A, Rolland M, Boyer C, Papayannakos N. Fluid Flow Characteristics of String Reactors Packed with Spherical Particles. *Chem Eng Technol* 2011;**34**:208-16.
- [15] Baerns M, Behr A, Brehm A, Gmehling J, Hofmann H, Onken U et al. *Technische Chemie*. Weinheim: WILEY-VCH Verlag GmbH & Co. KGaA; 2006.
- [16] Haase S, Bauer T. New method for simultaneous measurement of hydrodynamics and reaction rates in a mini-channel with Taylor flow. *Chem Eng Journal* 2011;**176-77**:65-74.
- [17] Dixon AG. Wall and particle-shape effects on heat-transfer in packed beds. *Chem Eng Commun* 1988;**71**:217-37.
- [18] Paschedag AR. *CFD in der Verfahrenstechnik - Allgemeine Grundlagen und mehrphasige Anwendungen*. 1st ed. Weinheim: WILEY-VCH Verlag GmbH & Co. KGaA; 2004.
- [19] Rosner DE. *Transport Processes in Chemically Reacting Flow Systems*. 1st ed. Toronto: General Publishing Company Ltd.; 2000.
- [20] Ferziger JH, Peric M. *Numerische Strömungsmechanik*. 1st ed. Berlin Heidelberg: Springer-Verlag; 2008.
- [21] Ergun S. Fluid flow through packed columns. *Chem Eng Prog* 1952;**48** 89-94.
- [22] Reichelt W. Calculation of pressure-drop in spherical and cylindrical packings for single-phase flow. *Chem Ing Tech* 1972;**44**:1068-71.
- [23] Fand RM, Thinakaran R. The influence of the wall on flow through pipes packed with spheres. *J Fluid Eng-T Asme* 1990;**112**:84-8.
- [24] Fand RM, Sundaram M, Varahasamy M. Incompressible fluid-flow through pipes packed with spheres at low dimension ratios. *J Fluid Eng-T Asme* 1993;**115**:169-72.

[25] Foumeny EA, Benyahia F, Castro JAA, Moallemi HA, Roshani S. Correlations of pressure-drop in packed-beds taking into account the effect of confining wall. *Int J Heat Mass Tran* 1993;**36**:536-40.

[26] Eisfeld B, Schnitzlein K. The influence of confining walls on the pressure drop in packed beds. *Chem Eng Sci* 2001;**56**:4321-9.

[27] Cheng NS. Wall effect on pressure drop in packed beds. *Powder Technol* 2011;**210**:261-6.

## Appendix A. Pressure drop correlations for single-phase flow through a bed of spheres with a low D/d ratio

$$\frac{\Delta p}{L} = f_{bed} \cdot \frac{1-\varepsilon}{\varepsilon^3} \frac{\rho \cdot u_0^2}{d} \left( 1 + \frac{2}{3} \frac{d}{(1-\varepsilon)D} \right) \quad \text{with} \quad f_{bed} = \frac{K_1}{\text{Re}_{bed}} + K_2 \quad (11)$$

$$\text{Reichert [22]:} \quad K_1 = 150 \quad \text{and} \quad K_2 = \left[ \frac{1.5}{\left(\frac{D}{d}\right)^2} + 0.88 \right]^{-2} \quad (12)$$

$$\text{Cheng [27]:} \quad K_1 = \left[ 185 + 17 \cdot \left( \frac{\varepsilon}{1-\varepsilon} \right) \left( \frac{D}{D+d} \right)^2 \right] \frac{1}{\left( 1 + \frac{2}{3} \left( \frac{1}{1-\varepsilon} \right) \frac{d}{D} \right)^2} \quad (13)$$

$$K_2 = \left[ 1.3 \cdot \left( \frac{1-\varepsilon}{\varepsilon} \right)^{\frac{1}{3}} + 0.03 \left( \frac{D}{D+d} \right)^2 \right] \frac{1}{\left( 1 + \frac{2}{3} \left( \frac{1}{1-\varepsilon} \right) \frac{d}{D} \right)^2}$$